Supporting Information

High-energy asymmetric supercapacitors based on free-standing hierarchical Co-Mo-S nanosheets with enhanced cycling stability

Jayaraman Balamurugan,[a] Chao Li,[a] Shaik Gouse Peera,[a] Nam Hoon Kim,[a] and Joong Hee Lee [a, b]*

[a]Advanced Materials Institute of BIN Convergence Technology (BK21 Plus Global) & Dept. of BIN Convergence Technology, Chonbuk National University, Jeonju, Jeonbuk 561-756, Republic of Korea.

[b]Carbon Composite Research Centre, Department of Polymer –Nano Science and Technology, Chonbuk National University, Jeonju, Jeonbuk 561-756, Republic of Korea

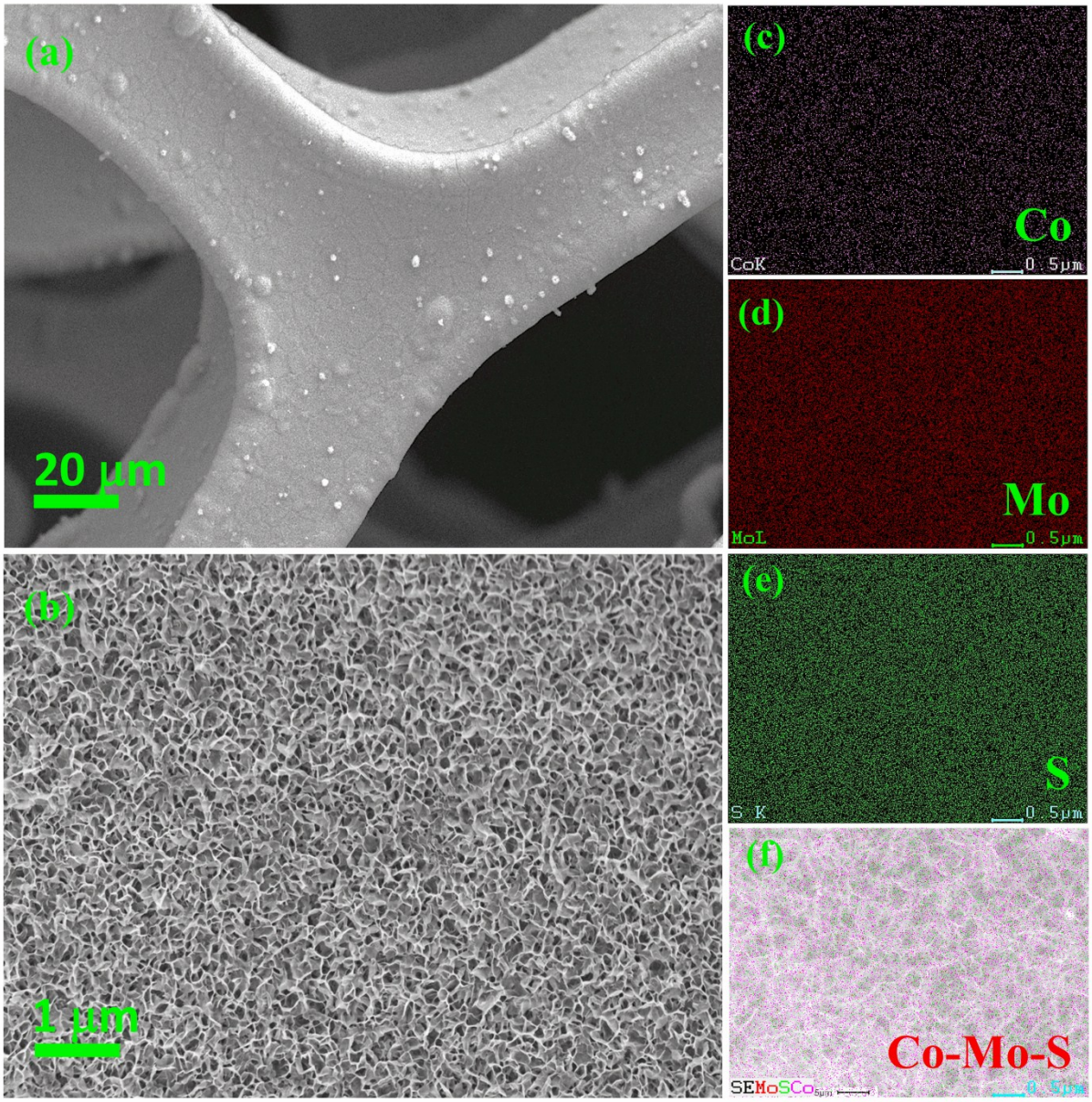

Fig. S1. (a, b) SEM pictures with different magnification of hierarchical Co-Mo-S NS and (c–f) corresponding EDS elemental mapping of Co-Mo-S NS.

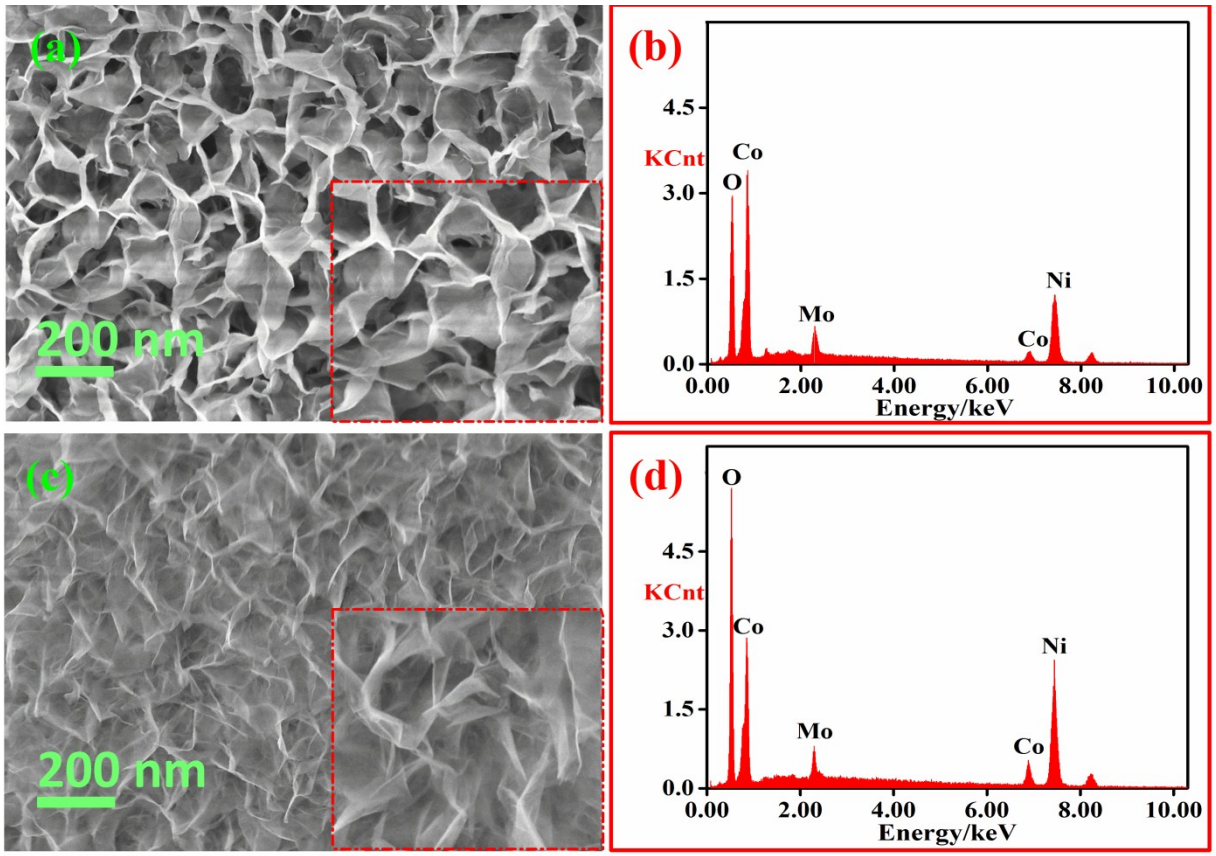

Fig. S2. (a) SEM image, (b) EDAX spectrum of Co-Mo LDH, (c) SEM image, and (d) EDAX spectrum of Co-Mo-O NS.

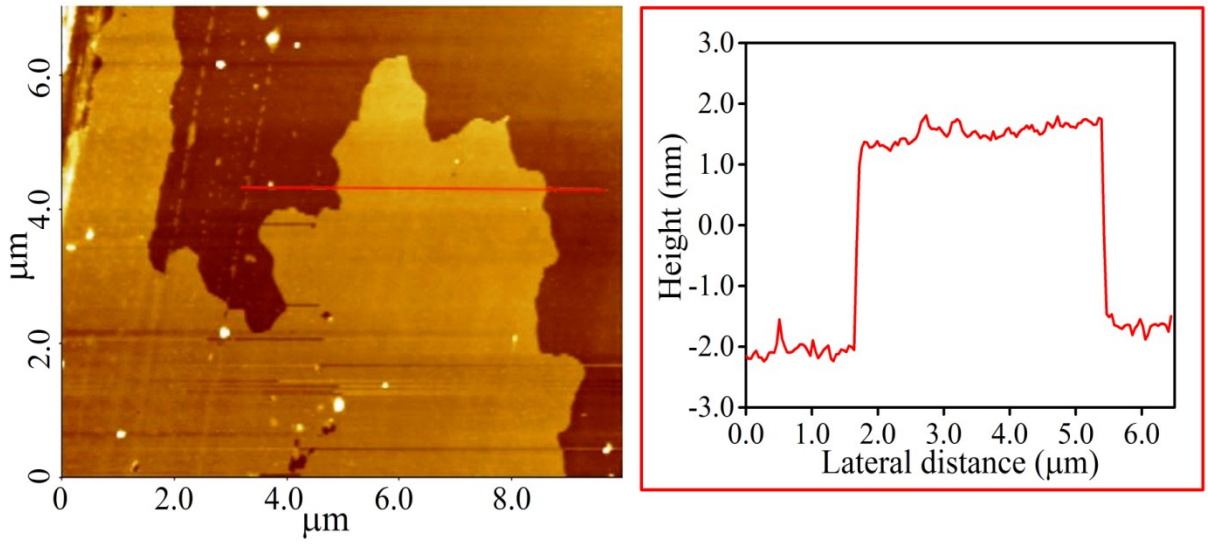

Fig. S3. AFM image and its height profile of hierarchical Co-Mo-S NS representing thickness of few nm and width > 3 μm.

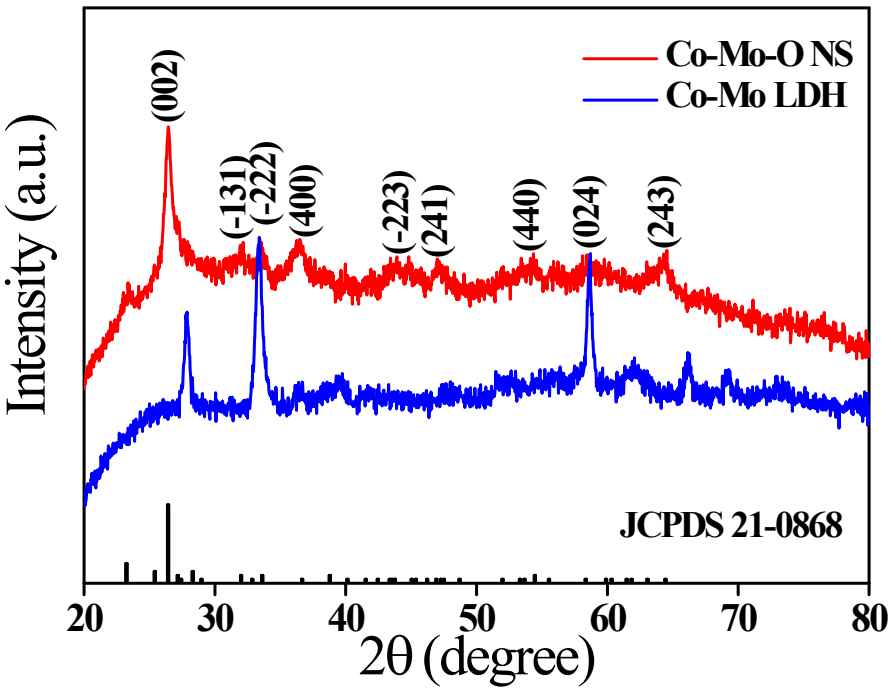

Fig. S4. XRD pattern of as-synthesized Co-Mo LDH and Co-Mo-O NS.

The XRD pattern of the Co-Mo LDH and Co-Mo-O NS are illustrated in Fig. S4. In case of the Co-Mo-O NS, the diffraction peaks at 2θ~26.4°, 31.9°, 33.6°, 36.3°, 43.9°, 47.0°, 53.9°, 58.5° and 64.5°, corresponding to the (002), (-131), (-222), (400), (-223), (241), (440), (024) and (243) planes of the monoclinic-phase for $CoMoO_4$ (JCPDS card no. 21-0868), respectively, suggesting that the excellent crystallinity of the $CoMoO_4$ NS architectures. In addition, the XRD pattern of Co-Mo LDH reveals that highly crystalline nature with multiple diffraction peaks with corresponding planes.

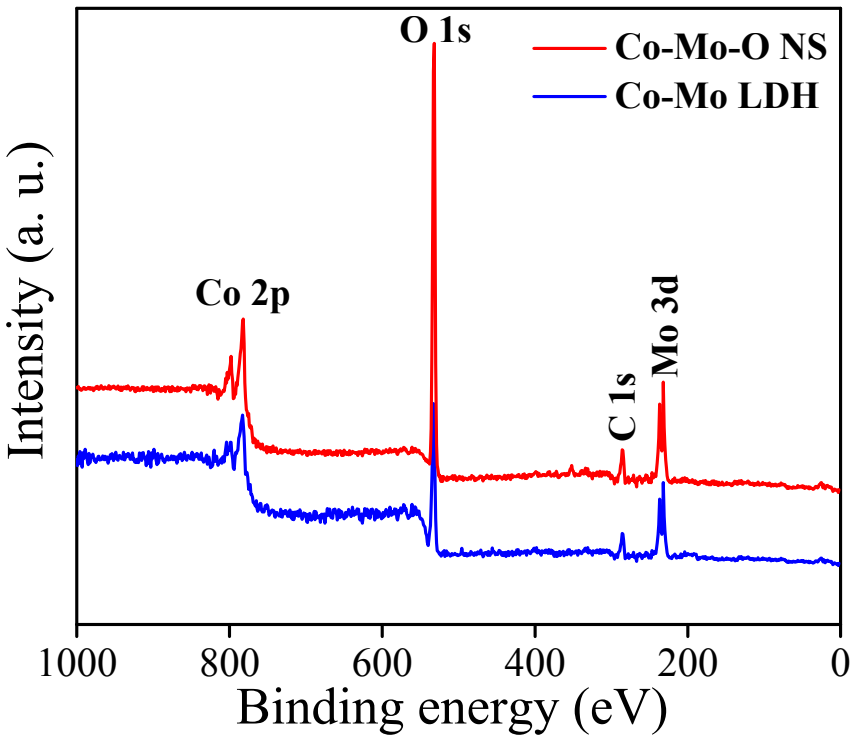

Fig. S5. XPS spectra of Co-Mo LDH and Co-Mo-O NS.

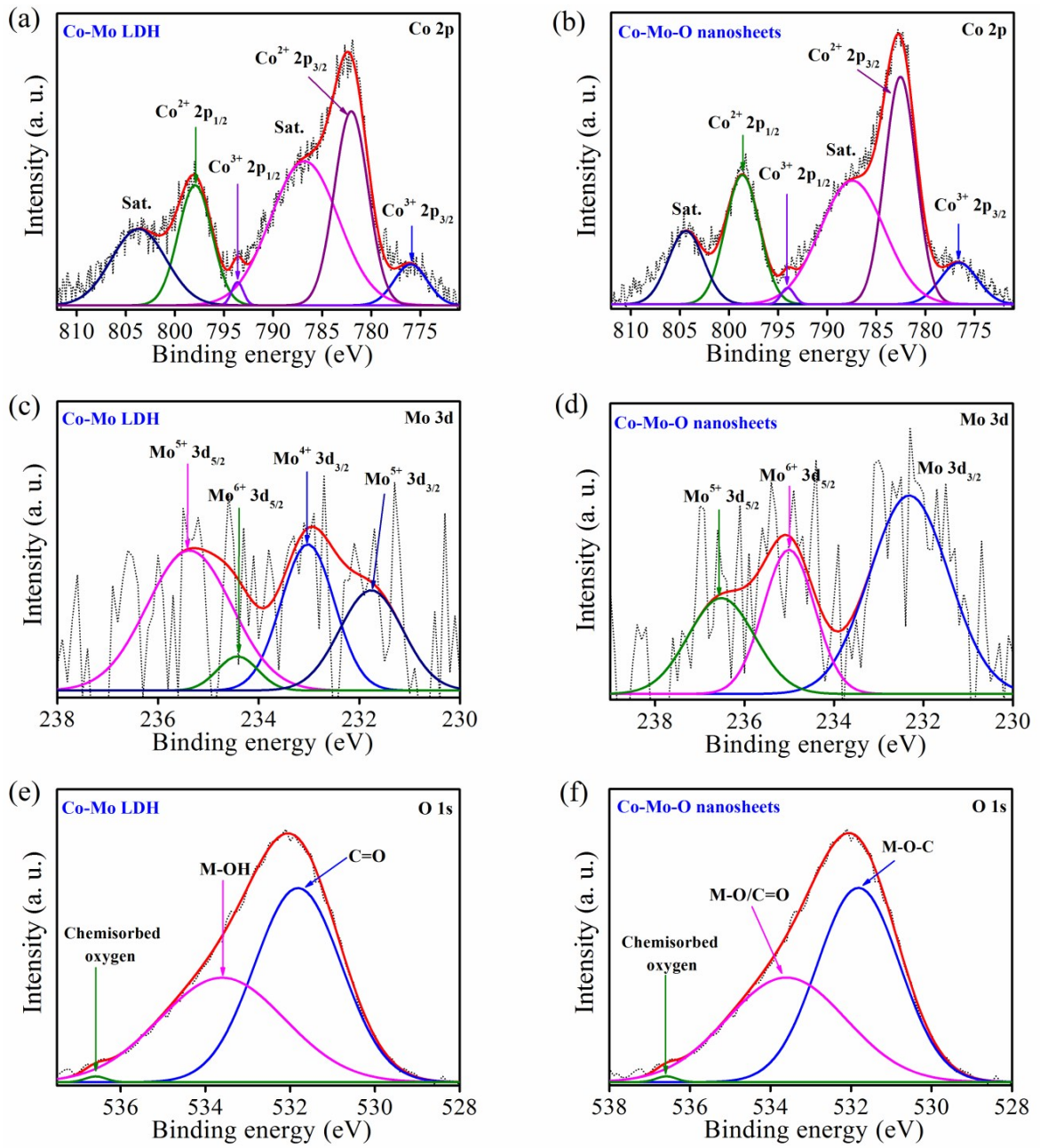

Fig. S6. (a, b) Co 2p spectra, (c, d) Mo 3d spectra, and (e, f) O 1s spectra of Co-Mo LDH and Co-Mo-O NS, respectively.

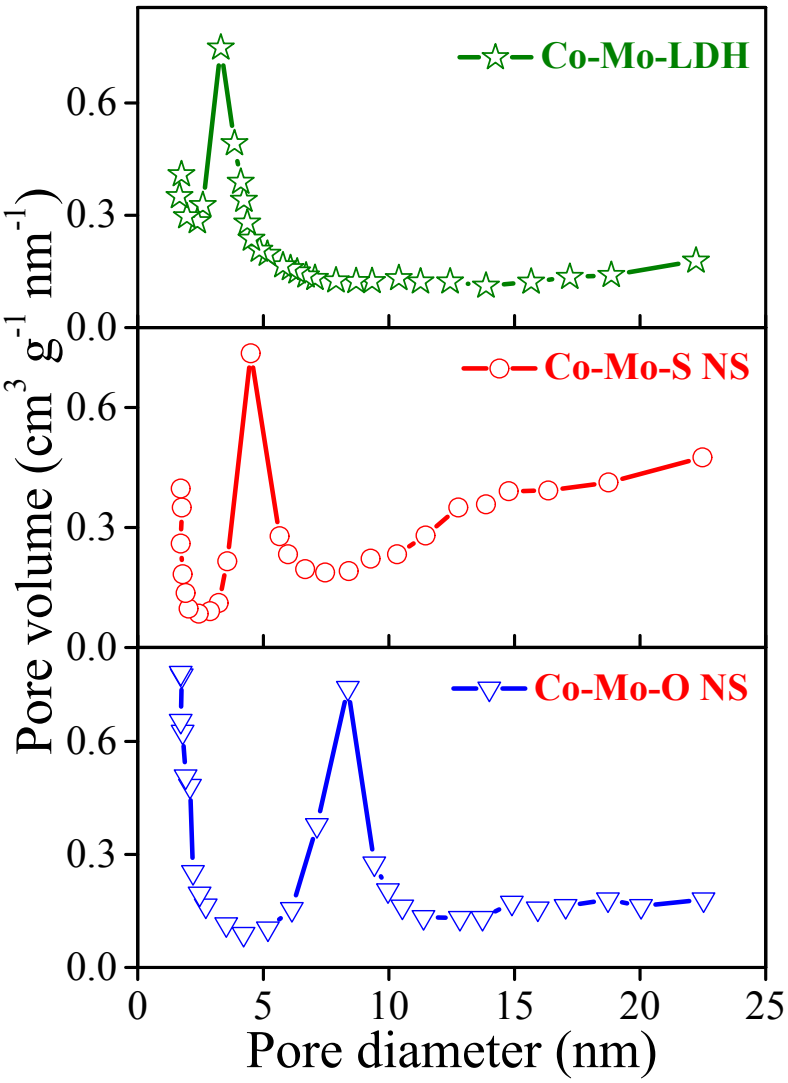

Fig. S7. Pore size distribution of as-synthesized Co-Mo LDH, Co-Mo-O and Co-Mo-S NS.

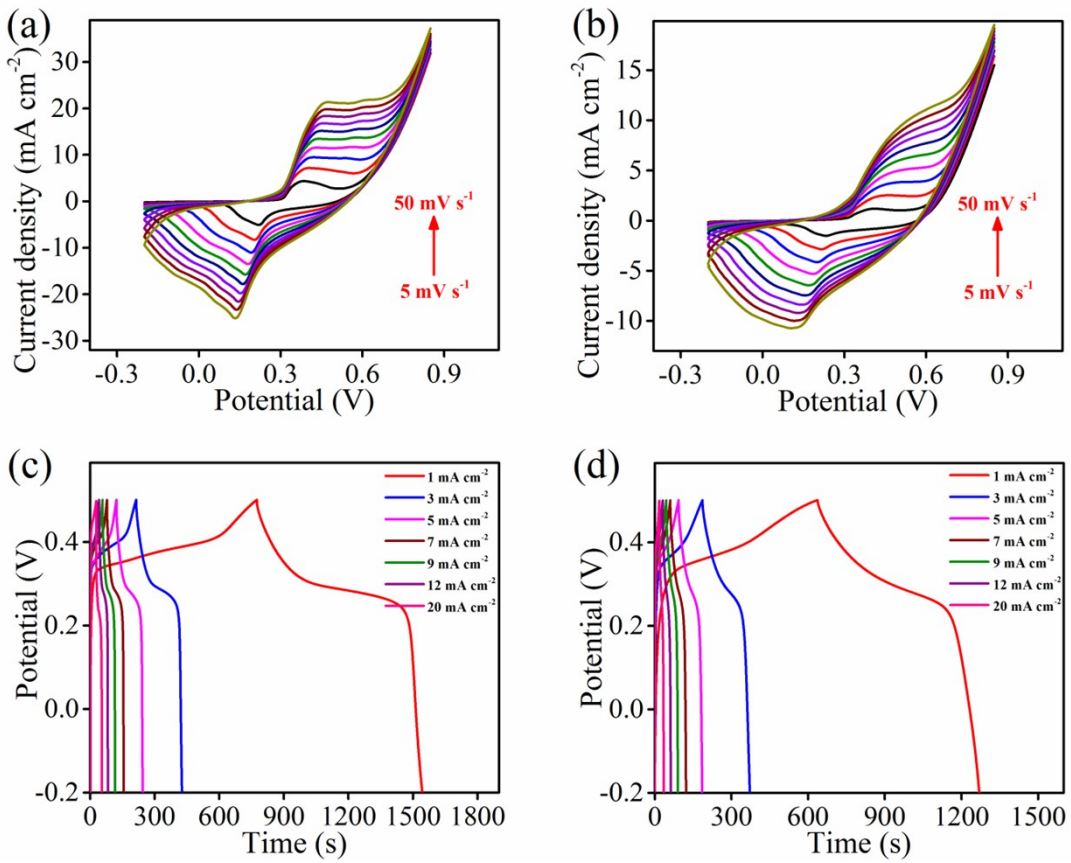

Fig. S8. CV curves of (a) Co-Mo LDH, (b) Co-Mo-O electrodes at the scan rate of 5–50 mV s^{-1}, GCD curves of (c) Co-Mo LDH, and (d) Co-Mo-O electrodes at the current densities of 1, 3, 5, 7, 9, 12 and 20 mA cm^{-2}.

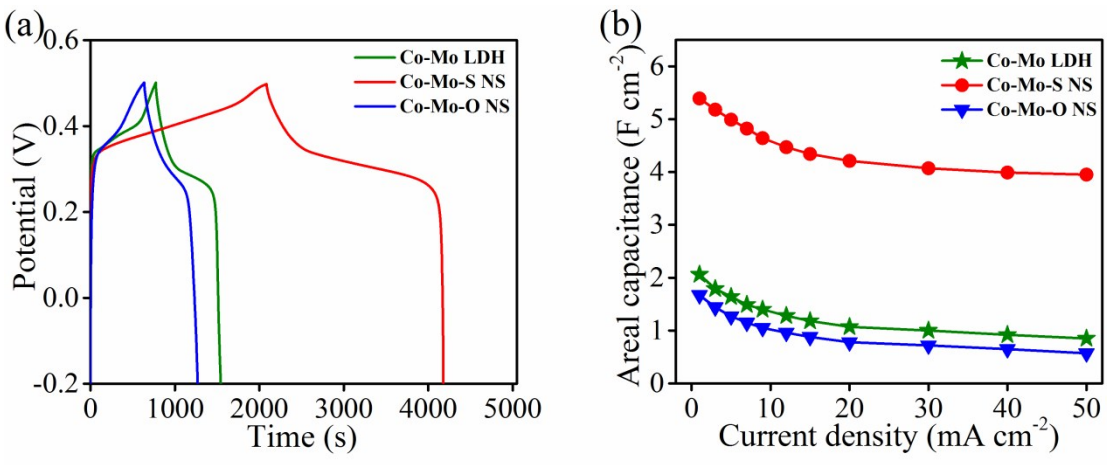

Fig. S9. (a) GCD curves of Co-Mo LDH, Co-Mo-O, and Co-Mo-S electrodes at the current density of 1 mA cm^{-2}, (b) Areal capacitance *vs.* current density of Co-Mo LDH, and Co-Mo-O, and Co-Mo-S electrodes.

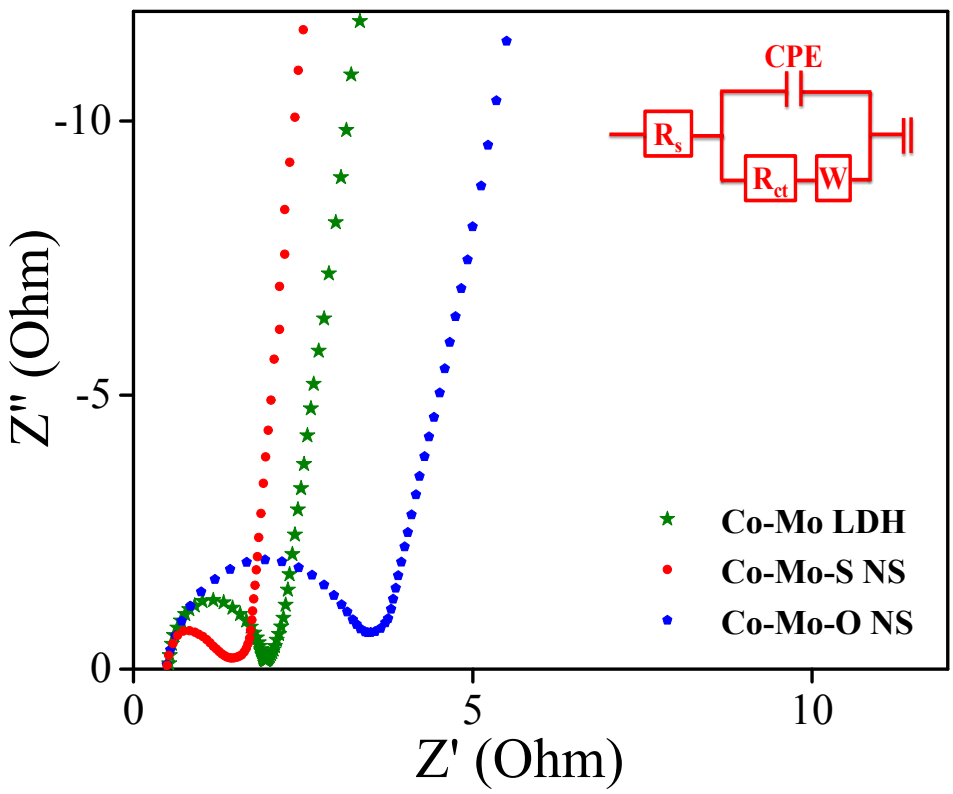

Fig. S10. EIS of Co-Mo LDH, Co-Mo-O, and Co-Mo-S electrodes.

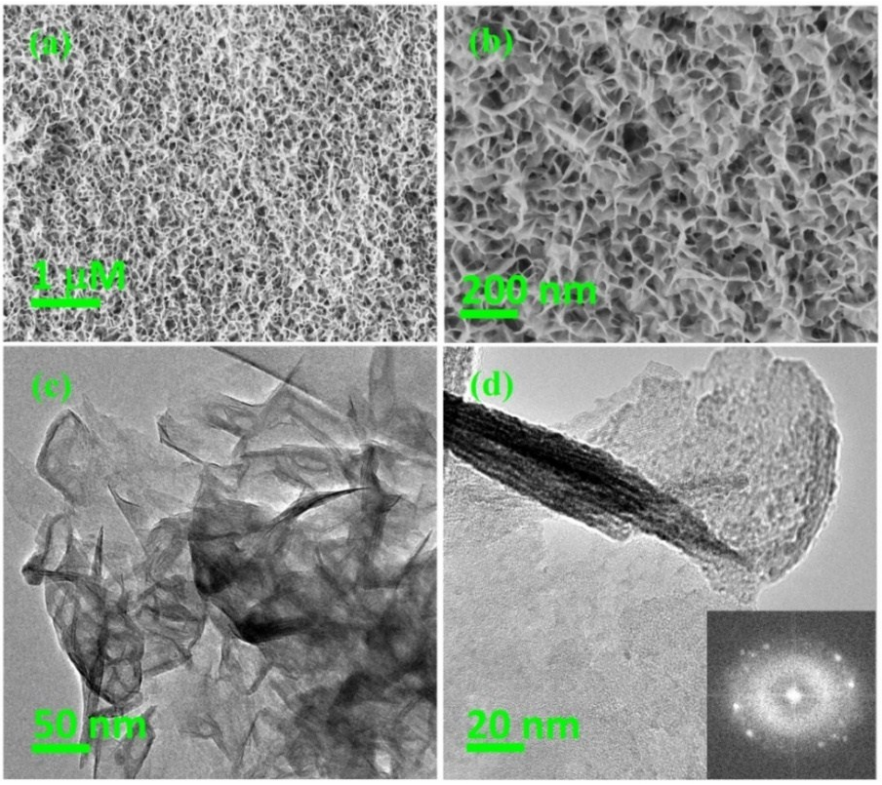

Fig. S11. (a, b) SEM images with different magnifications, and (c, d) low and high magnification TEM images of the Co-Mo-S NS, inset showing SAED pattern of Co-Mo-S NS (after stability test).

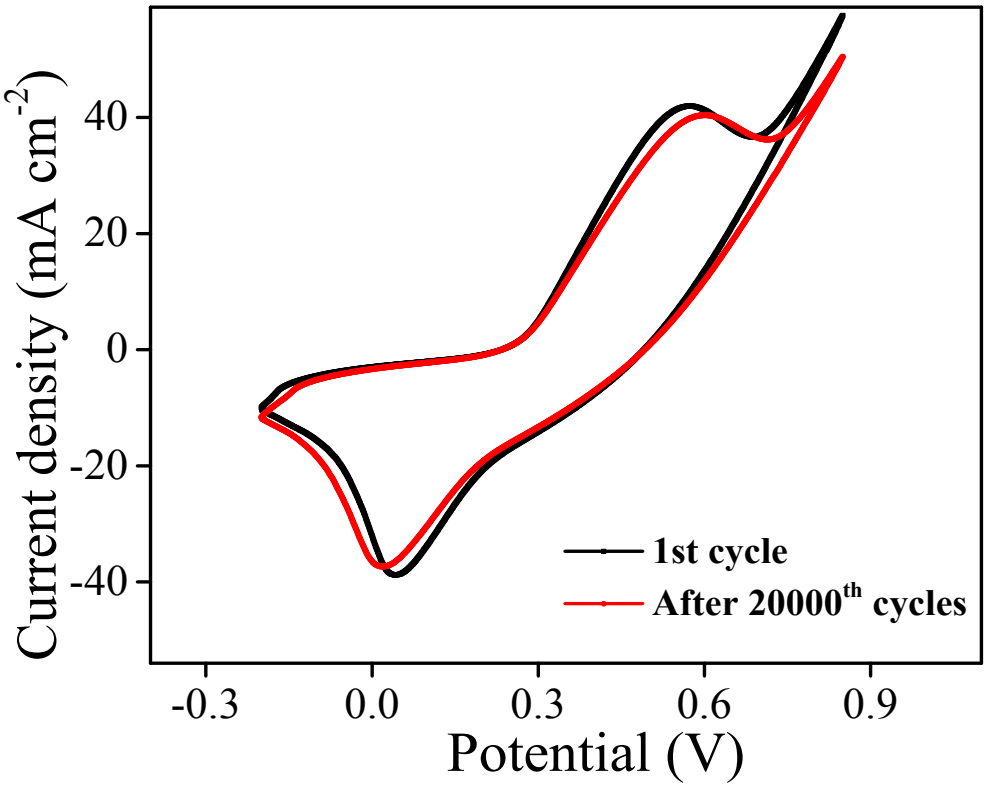

Fig. S12. CV curves of the Co-Mo-S electrode at 20 mV s^{-1} (before and after stability test).

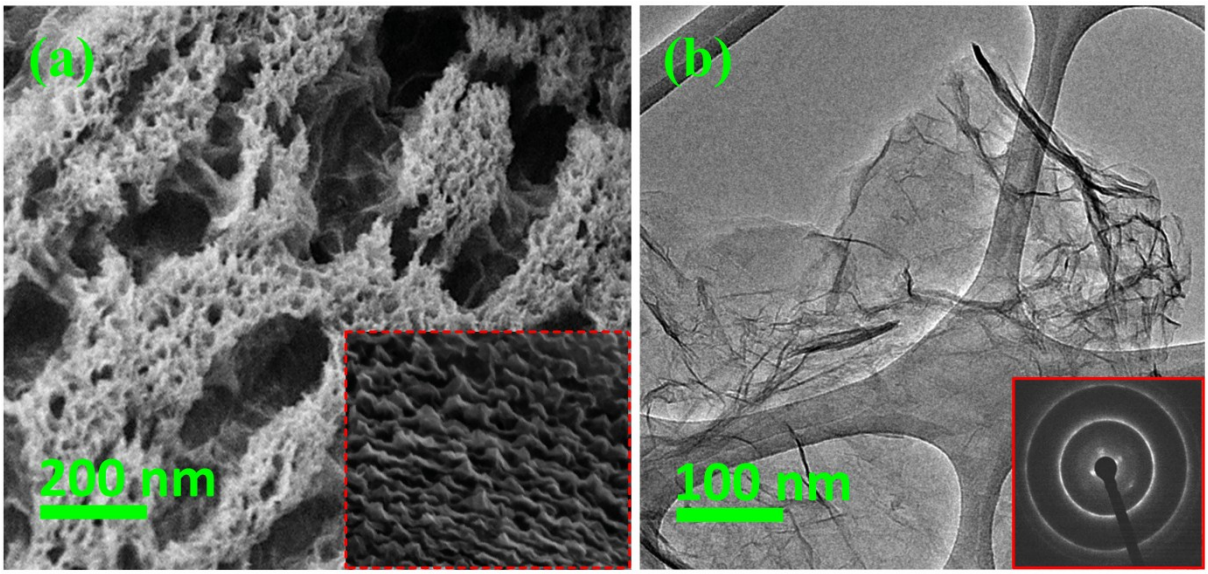

Fig. S13. (a) SEM image, (b) TEM image of NGNS, inset showing SAED pattern of NGNS.

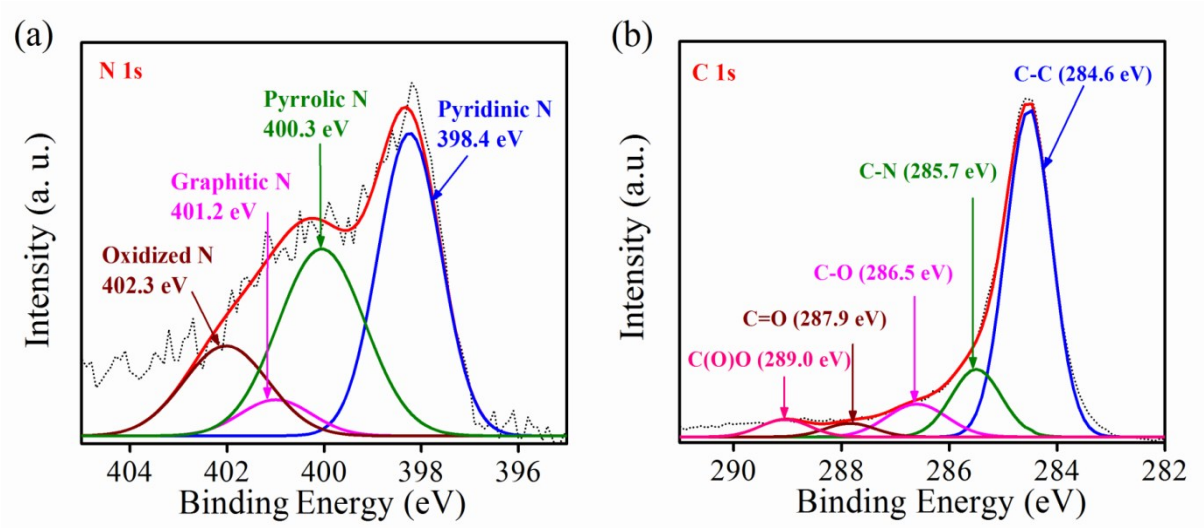

Fig. S14. High-resolution XPS of (a) N 1s, and (b) C 1s spectra for NGNS.

Typical XPS spectra of as-prepared NGNS are shown in Figure S14. The chemical compositions of the NGNS was calculated by taking C 1s, N 1s and O 1s and their atomic sensitivity factors into account. The composition ratios of C, N and O of this as-prepared NG material are 83.56%, 8.89%, and 7.55%, respectively. The deconvolution analysis of N 1s spectrum of NGNS (Fig. S14a) is composed of pyridine N, pyrrolic N, graphitic N, and oxidized N at 398.4, 400.3, 401.2 and 402.3 eV, respectively.[1] The broad pyridinic peak attributed from the nitrogen binds with two neighboring sp^2 carbon atoms of the graphene matrices.[2] This result confirms that the successful doping and introduction of N functional groups into graphene network, which is well-consistent with the previous reportes.[3, 4] In the C 1s spectrum of NG (Fig. S14b), deconvolution of the core-level C 1s spectrum shows five types of carbon bonds: sp^2 and sp^3 C–C (~284.6 eV), C–N (~285.7 eV), C–O (~286.5 eV), C=O (~287.9 eV), and C(O)O (~289.0 eV).

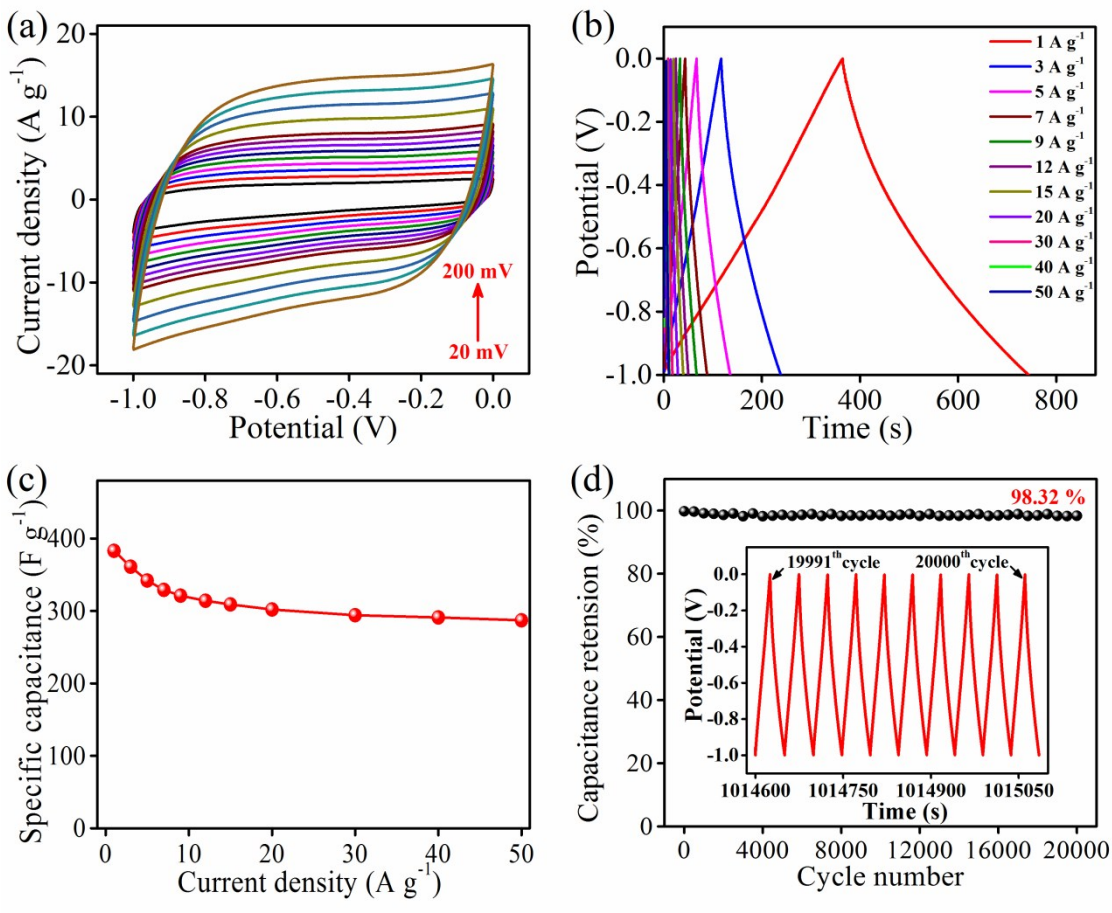

Fig. S15. Electrochemical properties of the NGNS: (a) CV curves of NGNS at different scan rates from 20 to 200 mV s^{-1}, (b) GCD curves of NGNS at different current densities of 1–50 A g^{-1}, (c) Specific capacitance *vs* current density of the NGNS electrode, and (d) Cycling performance of NGNS at a current density of 12 A g^{-1}, inset showing charge-discharge curves of NGNS electrode curves from 19991th to 20000th cycles.

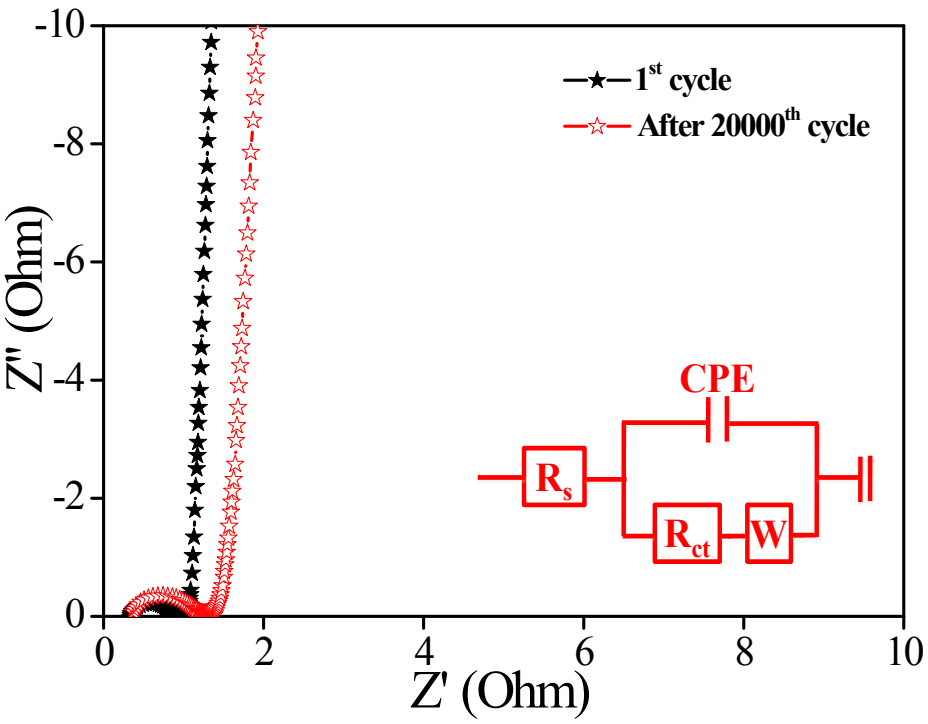

Fig. S16. EIS of NGNS electrode during the cycling performance.

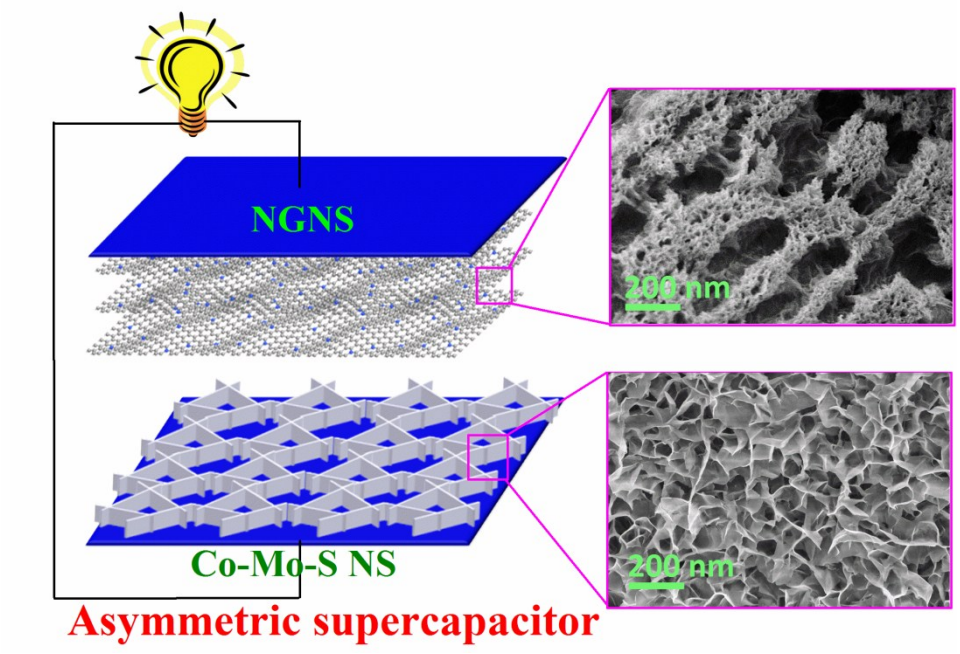

Fig. S17. Schematic illustration of the Co-Mo-S//NGNS ASC device.

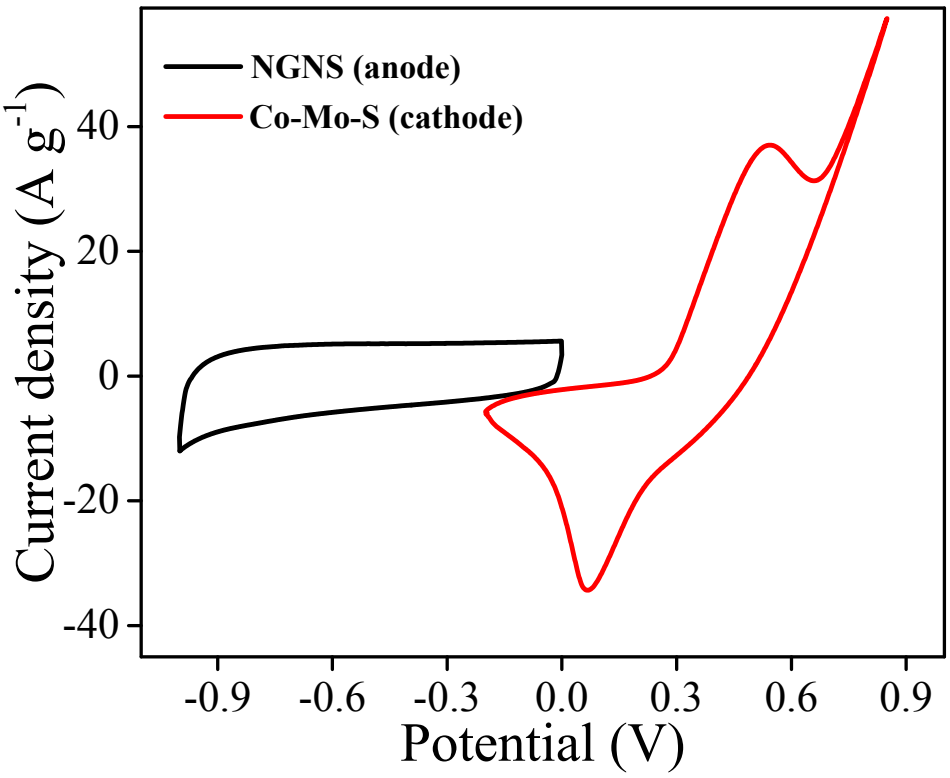

Fig. S18. Co-Mo-S (cathode) and NGNS (anode) measured at a scan rate of 20 mV s^{-1} in a three-electrode cell configuration.

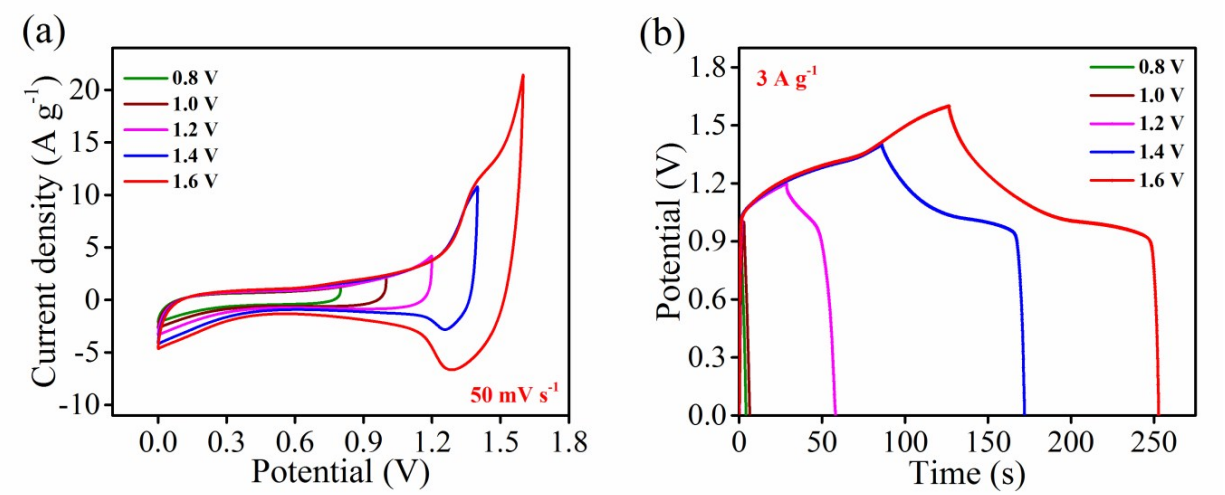

Fig. S19. CV curves of the ASC with different potential windows form 0.8–1.6 V at the scan rate of 50 mV s^{-1}, (b) GCD curves of the ASC with different potential windows form 0.8–1.6 V at the current density of 3 A g^{-1}.

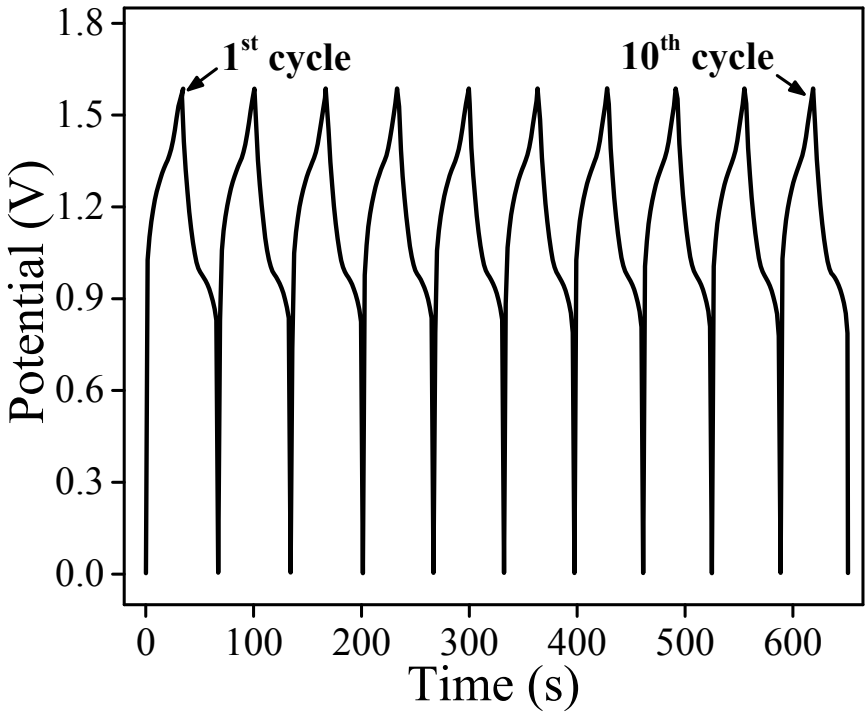

Fig. S20. GCD curves of ASC during the cycling performance (from the 1st to 10th cycles).

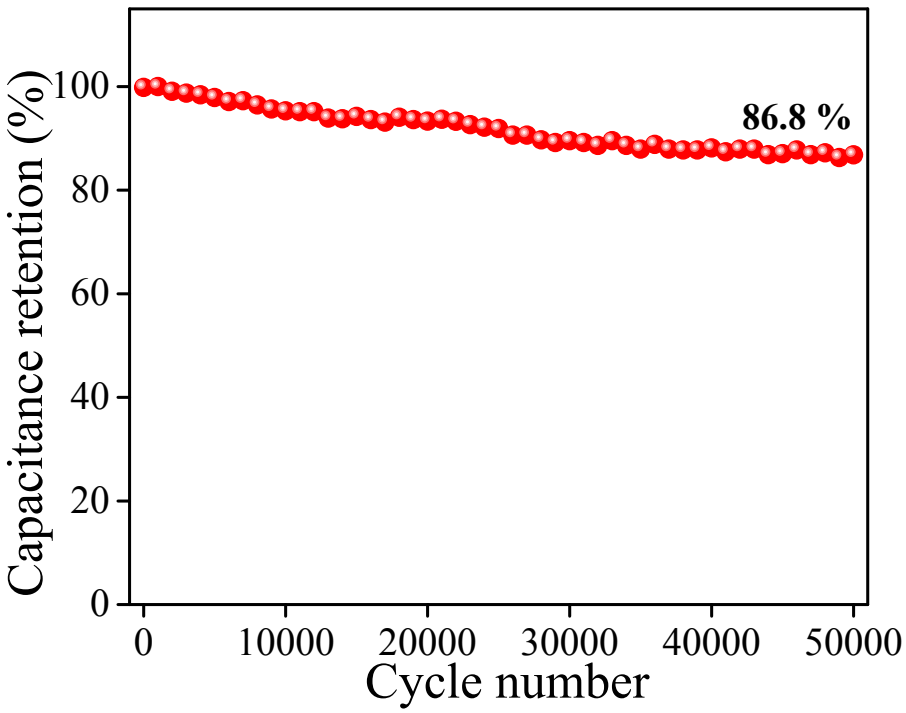

Fig. S21. Cycling performance of ASC at the current density of 10 A g^{-1} (up to 50000 cycles).

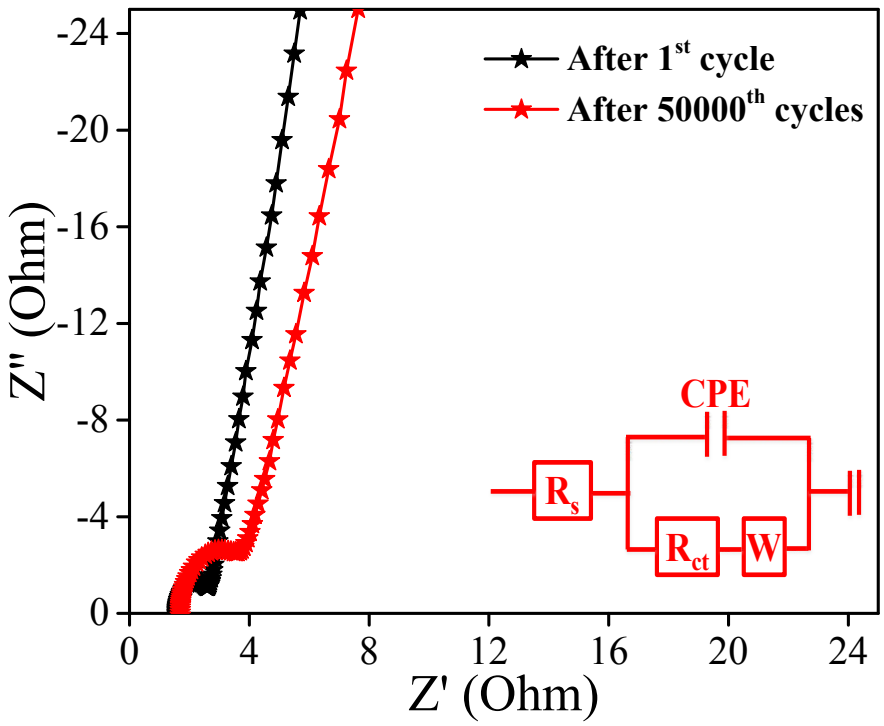

Fig. S22. Nyquist impedance spectra of ASC during the cycling performance (before and after stability test).

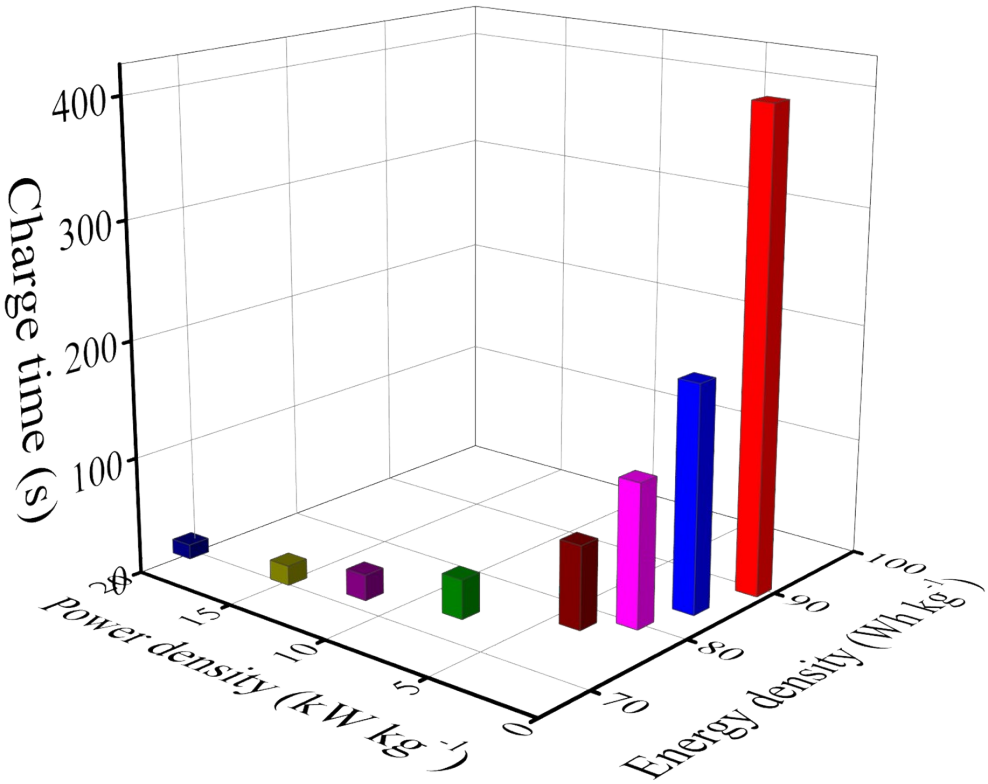

Fig. S23. Regone plot (energy density *vs.* power density *vs.* charge time) of ASC device.

Table S1. Elemental composition of Co-Mo LDH, Co-Mo-O, and Co-Mo-S NS estimated from XPS and ICP-AES.

Sample	Co (at. %)	Mo (at. %)	S (at. %)	O (at. %)
Co-Mo LDH	32.85	31.49	-	23.98
Co-Mo-O NS	31.18	30.82	-	31.36
Co-Mo-S NS	32.56	31.09	23.21	9.97

Co, Mo, S and O contents were detected by XPS analysis and ICP-AES measurements.

Table S2. Electrochemical properties of the hierarchical Co-Mo-S NS comparison with reported transition metal sulfides based electrodes.

Materials	Specific capacitance (F g^{-1})	Areal capacitance (F cm^{-2})	Current load or scan rate	Electrolyte	Stability	References
Co_9S_8/Ni foam	1645	–	3 A g^{-1}	2 M KOH	94.4% (2000 cycles)	5
CoS_2 hollow sphere	1301	–	1 A g^{-1}	2 M KOH	90.1% (2000 cycles)	6
CoS_2 nanowire	828	1.27	0.01V s^{-1}	6 M KOH	97.5% (4250 cycles)	7
MoS_2 nanosheets	589	–	0.5 A g^{-1}	1M H_2SO_4	104% (2000 cycles)	8
MoS_2/PPy	695	–	0.5 A g^{-1}	1 M KCl	85% (4000 cycles)	9
MoS_2@PANI	853	–	1 A g^{-1}	0.5 M H_2SO_4	91% (4000 cycles)	10
Ni_3S_2@MoS_2 core-shell NR	848	–	5 A g^{-1}	2 M KOH	91% (2000 cycles)	11
Ni_3S_4@MoS_2 core-shell NS	1441	–	2 A g^{-1}	6 M KOH	90.7 % (3000 cycles)	12
$NiCo_2S_4$ hollow spheres	1036	–	1 A g^{-1}	6 M KOH	87 % (2000 cycles)	13
$NiCo_2S_4$ hollow nanotubes	1154	–	1 A g^{-1}	2 M KOH	92.8 % (8000 cycles)	14
Ni-Co-S	1418	–	5 A g^{-1}	1 M KOH	-	15
$FeCo_2S_4$–$NiCo_2S_4$ composite	1519	3.50	5 mA cm^{-2}	3 M KOH	95.1% (5000 cycles)	16
Co-Mo-S NS	2343	5.39	1 mA	3 M KOH	96.6 %	Present

	cm^{-2}	(20000 cycles)	work

Table S3. ASCs Device properties comparison with reported literatures.

Reported ASC Device	Electrolyte	Device Window (V)	Energy Density (Wh kg^{-1})	Power Density (W kg^{-1})	Stability (Cycle No.)	Reference
CoS/Graphene//AC	2M KOH	0-1.6	29	800	70% (10000 cycles)	17
MnO_2/GNS //MoS_2/GNS	PVA/Na_2SO_4 gel electrolyte	0-2.0	78.9	284.1	90 % (5000 cycles)	18
Ni-Co-S/G//PCNS	6 M KOH	0-1.6	43.3	800	85% (10000 cycles)	19
$NiCo_2S_4$/NCF//OMC/NCF	6 M KOH	0-1.6	45.5	512	70.4% (10000 cycles)	20
$FeCo_2S_4$//3D PNG	KOH/PVA gel electrolyte	0-1.6	76.1	755	82% (10000 cycles)	21
$CuCo_2S_4$–HNN//AC	3 M KOH	0-1.6	44.1	800	94.1% (6000 cycles)	22
$NiMoO_4$//AC	2 M KOH	0-1.7	60.9	850	85.7% (10000 cycles)	23
Co_3O_4@$CoMoO_4$//CNTs	PVA/ KOH	0-1.6	45.2	400	98.5% (3000 cycles)	24
$CoMoO_4$@$NiMoO_4$//AC	2 M KOH	0-1.6	28.7	267	99% (3000 cycles)	25
Co-Mo-S//NGNS	PVA/KOH	0-1.6	89.6	789	86.5% (50000 cycles)	Present work

Notes and references

1. D. Wei, Y. Liu, Y. Wang, H. Zhang, L. Huang and G. Yu, *Nano Lett*., 2009, **9**, 1752-1758.
2. B. Stohr, H. P. Boehm and R. Schlogl, *Carbon*, 1991, **29**, 707-720.
3. K. Parvez, S. Yang, Y. Hernandez, A. Winter, A. Turchanin, X. Feng and K. Mullen, *ACS Nano*, 2012, **6**, 9541-9550.
4. Z. Wen, X. Wang, S. Mao, Z. Bo, H. Kim, S. Cui, G. Lu, X. Feng and J. Chen, *Adv. Mater*., 2012, **24**, 5610-5616.
5. H. Li, Y. Gao, Y. Shao, Y. Su and X. Wang, *Nano Lett.,* 2015, **15**, 6689-6695.
6. S. Peng, L. Li , H. Tan, R. Cai, W. Shi, C. Li, S. G. Mhaisalkar, M. Srinivasan, S. Ramakrishna and Q. Yan, *Adv. Funct. Mater.*, 2014, **24**, 2155-2162.
7. R. Ren, M. S. Faber, R. Dziedzic, Z. Wen, S. Jin, S. Mao and J. Chen, *Nanotechnology*, 2015, *26*, 494001.
8. H. Ji, C. Liu, T. Wang, J. Chen, Z. Mao, J. Zhao, W. Hou and G. Yang, *Small*, 2015, **11**, 6480-6490.
9. H. Tang, J. Wang, H. Yin, H. Zhao, D. Wang and Z. Tang, *Adv. Mater.,* 2015, **27**, 1117-1123.
10. J. Zhu, W. Sun, D. Yang, Y. Zhang, H. H. Hoon, H. Zhang and Q. Yan, *Small*, 2015, **11**, 4123-4129.
11. J. Wang, D. Chao, J. Liu, L. Li, L. Lai, J. Lin and Z. Shen, *Nano Energy,* 2014, **7**, 151-160.
12. Y. Zhang, W. Sun, X. Rui, B. Li, H. T. Tan, G. Guo, S. Madhavi and Y. Zong, Q. Yan, *Small,* 2015, **11**, 3694-3702.
13. L. Shen, L. Yu, H. B. Wu, X. Y. Yu, X. Zhang and X. W. Lou, *Nat. Commun.*, 2015, **6**, 6694-6701.
14. X. Xiong, G. Waller, D. Ding, D. Chen, B. Rainwater, B. Zhao, Z. Wang and M. Liu, *Nano Energy*, 2015, **16**, 71-80.

15. W. Chen, C. Xia and H. N. Alshareef, *ACS Nano,* 2014, **8**, 9531-9541.

16. J. Zhu, S. Tang, J. Wu, X. Shi, B. Zhu and X. Meng, *Adv. Energy Mater.* **2016**, 1601234.

17. J. Shi, X. Li, G. He, L. Zhang and M. Li, *J. Mater. Chem. A*, 2015, **3**, 20619-20626.

18. X. Yang, H. Niu, H. Jiang, Q. Wang and F. Qu, *J. Mater. Chem. A*, **2016**, *4*, 11264-11275.

19. J. Yang, C. Yu, X. Fan, S. Liang, S. Li, H. Huang, Z. Ling, C. Hao and J. Qiu, *Energy Environ. Sci.*, 2016, **9**, 1299-1307.

20. L. Shen, J. Wang, G. Xu, H. Li, H. Dou and X. Zhang, *Adv. Energy Mater.*, 2015, **5**, 1400977.

21. S. Tang, B. Zhu, X. Shi, J. Wu and X. Meng, *Adv. Energy Mater.*, 2017, **7**, 1601985.

22. S. E. Moosavifard, S. Fani and M. Rahmanian, *Chem. Commun.*, 2016, **52**, 4517-4520.

23. S. Peng, L. Li, H. Wu, S. Madhavi and X. W. Lou, *Adv. Energy Mater.*, 2015, **5**, 1401172.

24. J. Wang, X. Zhang, Q. Wei, H. Lv, Y. Tian, Z. Tong, X. Liu, J. Hao, H. Qu, J. Zhao, Y. Li and L. Mai, *Nano Energy*, 2016, **19**, 222-233.

25. Z. Zhang, H. Zhang, X. Zhang, D. Yu, Y. Ji, Q. Sun, Y. Wang and X. Liu, *J. Mater. Chem. A*, 2016, **4**, 18578-18584.